Simulation of Solid Movement during Solidification by a Simple Multiphase Approach

A. Ludwig, G. Ehlen, M. Pelzer, P.R. Sahm
Foundry Institute, RWTH-Aachen
Intzestr. 5, D-52056 Aachen, Germany

Abstract

A two-phase approach is used to describe the movement of solid during equiaxed solidification of castings. This approach considers the growing solid as a separate continuous phase for which the conservation of mass, momentum, species and enthalpy can be expressed by the corresponding differential equations with source and exchange terms. Thus sedimentation and/or floating of solid during solidification can be described. The essential model considerations are represented by the choice of the exchange terms. In contrast to recent publications, simple exchange terms describing the basic proceedings during alloy solidification are used in the present work. It is shown, how the choice of different mass transfer rates and momentum exchange terms influences the global evolution of temperature, velocity and concentration during the beginning of equiaxed solidification.

Modeling of Casting, Welding and Advanced Solidification Processes IX
Edited by Peter R. Sahm, Preben N. Hansen and James G. Conley

1. Introduction

A very promising approach for the numerical description of the microstructure evolution during alloy solidification considering nucleation, growth and movement of grains was recently presented by C. Beckermann and C.Y. Wang [1,2]. They used a two-phase model assuming that both phases, liquid and solid, can be described as a continuous phase with its own velocity and average species concentration. However, due to several sophisticated details, their model has a lot of empirical parameters for which the used values seem to be somehow artificial. In the present paper a two-phase model is presented where a simple approach for the mass, solute and momentum transfer rate is used. Only three empirical parameters are introduced. The impact of the chosen values of these parameters on the solidification process of Al-4wt.%Cu is discussed.

2. Model Description

A multi-phase flow can be modeled by considering each of several phases as a continuum and applying the conservation of mass, momentum, enthalpy and species for each of them. It is thought that the corresponding quantities represent the mean values averaged over a control volume. The corresponding equations are:

mass:
$$\frac{\partial}{\partial t}(\alpha_q \rho_q) + \nabla \cdot (\alpha_q \rho_q \vec{u}_q) = M_{pq} \tag{1}$$

momentum:
$$\frac{\partial}{\partial t}(\alpha_q \rho_q \vec{u}_q) + \nabla \cdot (\alpha_q \rho_q \vec{u}_q \otimes \vec{u}_q) = -\alpha_q \nabla p + \nabla \cdot \bar{\bar{\tau}}_q + \alpha_q \rho_q \vec{g} + U_{pq} \tag{2}$$

solute:
$$\frac{\partial}{\partial t}(\alpha_q \rho_q c_q^i) + \nabla \cdot (\alpha_q \rho_q \vec{u}_q c_q^i) = \nabla \cdot (\alpha_q \rho_q D_q^i \nabla c_q^i) + C_{pq}^i \tag{3}$$

enthalpy:
$$\frac{\partial}{\partial t}(\alpha_q \rho_q h_q) + \nabla \cdot (\alpha_q \rho_q \vec{u}_q h_q) = -\nabla \vec{q}_q + H_q \tag{4}$$

where α_q is the volume fraction, ρ_q the physical density, $\vec{u}_q$ the velocity, τ_q the strain tensor, and h_q the enthalpy of phase q. $\vec{q}_q$ the heat flux in phase q. c_q^i is the mass fraction and D_q^i the diffusivity of the i-th species in phase q. $\vec{g}$ is the gravitation vector and p the pressure. In this work the phases liquid and solid ($q = l, s$) are considered.

An essential feature of the present model is the consideration of source and exchange terms in the conservation equations. The exchange terms for the continuity equations M_{ls} and M_{sl} account for the phase change from liquid to solid and vice versa. Momentum exchange between the solid and the liquid phase is described by the exchange terms U_{ls} and U_{sl} in the momentum conservation equations. Segregation phenomena during solidification are to be incorporated in the exchange terms of the conservation equations for species mass fraction C_{ls}^i and C_{sl}^i. The difference in enthalpy between solid and liquid (heat of fusion) leads to source terms H_l and H_s in the enthalpy conservation equations. As the exchange and source terms are the essential part of the present work further details are given in sections 2.1 – 2.4.

To solve the conservation equations the density ρ_q, the diffusion coefficient D_q, and the viscosity μ_q must be defined and known for each phase. The viscosity of the solid phase is chosen so that the liquid/solid mixture reveals the empirically known viscosity of a liquid/granular mixture [3]. This approach was adopted from [1,4]. For small granular (solid) fraction α_s the viscosity of the mixture is governed by μ_l. With increasing α_s, the viscosity of the mixture μ_{mix} increases rapidly. For

$\alpha_s = \alpha_s^c \approx 0{,}637$ the solid phase is closely packed and further flow of the mixture is impossible. At that point μ_{mix} is infinity. With $\mu_{mix} = \alpha_l \mu_l + \alpha_s \mu_s$ the described behavior is reproduced by [3]

$$\mu_s = \frac{\mu_l}{\alpha_s} \cdot \left(\left(1 - \alpha_s / \alpha_s^c\right)^{-2{,}5 \cdot \alpha_s^c} - (1 - \alpha_s) \right) \tag{5}$$

2.1 Mass transfer

After solving Eq. (1)-(4) for both, the liquid and the solid phase, the temperature T and the (average) species mass fraction of Cu in the liquid c_l^{Cu} is known at each nodal point within the domain. It is now assumed that the average temperature at the solid/liquid interface is given by the equilibrium phase diagram. From this assumption, the average species mass fraction (concentration) in the liquid at the interface is given by $c_l^{Cu^*} = (T - T_f)/m$, where T_f is the melting point of the solvent and m is the slope of the liquidus line. Due to the existing segregation around the growing solid phase, this species mass fraction is generally higher than the average species mass fraction within the control volume c_l^{Cu}. The difference between $c_l^{Cu^*}$ and c_l^{Cu} is thought to be the driving force for the phase change and thus used to define the mass transfer between liquid and solid:

$$M_{ls} = g_\alpha \cdot \left(\frac{T - T_f}{m} - c_l^{Cu} \right) \tag{6}$$

g_α is an empirical constant. This formulation treats solidification and melting symmetrically. Note that this approach neither accounts for the present morphology of the growing solid nor for the diffusion around dendrite tip regions. Its advantage is the extreme simplicity which, by changing the value of g_α, can help to investigate the necessary precision of a mass transfer model regarding the impact on the solidification process and the final macrosegregation pattern. Similar to single phase solidification, the mass transfer during the eutectic reaction is modeled by

$$M_{ls} = g_{Eut} \cdot (T_E - T). \tag{7}$$

Here T_E is the eutectic temperature and g_{Eut} the corresponding empirical constant. Note that the results presented in this paper are for the beginning of the solidification process only. Therefore the impact of g_{Eut} on the simulation results will be discussed in a subsequent paper.

2.2 Momentum transfer

The choice of an adequate model for the momentum exchange between moving dendritic grains and the flowing melt is subject of ongoing scientific discussions [5]. In this work two mechanisms for the momentum exchange between the solid and the liquid phase are considered: friction and phase change. The friction-approach is based on Darcy's law [7] and on the Blake-Kozeny equation [7] for an isotropic permeability of the mushy zone. Thus, an exchange term of the form $U_{ls} = \alpha_l^2 \mu_l K_{isotr}^{-1} (\bar{u}_l - \bar{u}_s)$ is introduced with a permeability given by:

$$K_{isotr} = K_0 (\alpha_l^3 / \alpha_s^2) \tag{8}$$

K_0 is an empirical parameter which can be used to study the impact of strong or weak momentum transfer on the flow pattern and therefore on the final macrosegregation.

The transfer from one to the other phase leads to a further momentum exchange mechanism. For solidification this mechanism is accounted for by adding (subtracting) the term $U_{ls} = M_{ls} \bar{u}_l$ to the momentum conservation equation of the solid (liquid). Remelting is accounted for by adding (subtracting) the term $U_{sl} = M_{sl} \bar{u}_s$ to the momentum conservation equation for the liquid (solid).

2.3 Heat of fusion

The different enthalpies of the liquid and the solid phase result in the following source terms for the enthalpy conservation equations: $H_l = -h_l M_{ls}$ and $H_s = h_s M_{ls}$. Note that these source terms give the heat of fusion as $\Delta h_f = h_s - h_l$.

2.4 Species transfer

It is assumed that during each time step the solid phase grows by adding a thin solid shell (not necessarily uniform in thickness) from the melt. The corresponding decrease of the liquid mass per volume and time is simply M_{ls}. Therefore the mass of Cu in the liquid per volume and time is reduced by $c_l^{Cu} M_{ls}$. From this Cu-mass, $k \cdot c_l^{Cu} M_{ls}$ is incorporated in the solid (k is the equilibrium distribution coefficient). Thus, the reduction of liquid Cu-mass by $c_l^{Cu} M_{ls}$ is partly compensated by the amount $(1-k) c_l^{Cu} M_{ls}$ which represents the Cu-mass not incorporated into the solid shell. In conclusion the source term for the conservation equation of species mass fraction in the solid phase has to be

$$C_{ls}^{Cu} = k \cdot c_l^{Cu} M_{ls} \tag{9}$$

and the negative equivalent for the liquid phase. Note that these sources do change the average mass fraction in the liquid and the solid, rather than the equilibrium ones, $c_l^{Cu^*}$ and $k c_l^{Cu^*}$, which are thought to exist in average at the solid/liquid interface.

2.5 Numerical Implementation

The conservation equations Eq. (1)-(4) for both, the liquid and the solid phase, are solved using a fixed-grid, single-domain numerical solution procedure. A fully implicit, control-volume based finite-difference method is utilized to discretize the equations, with the upwind scheme used to evaluate the finite-difference coefficients. The velocity-pressure coupling in the momentum equations is handled using the SIMPLE iteration technique [8]. The solution procedure was performed with the help of the commercial CFD-software FLUENT in the Eulerian-Eulerian multiphase mode.

3. Results and Discussion

The physical system of consideration is illustrated in Figure 1. An initially quiescent binary alloy of uniform temperature and concentration was assumed. A single wall is subject to convective cooling from a coolant at constant temperature and heat transfer coefficient. The remaining walls are considered to be adiabatic, with all walls assumed to be impermeable. The velocity boundary conditions are zero normal velocity component and a non-slip tangential velocity for both phases. At the top of the domain a zero diffusion flux condition is applied, which means that the conditions are extrapolated from within the domain. The thermophysical properties used for the simulations are given in Table 1. Note that the density of the liquid and the solid are assumed to be constant. Thus no thermo-solutal convection is considered.

ρ_L = 2606 kg/m^3	$c_{P,S}$ = 766 J/(kg·K)	T_l = 933.5 K
ρ_S = 2743 kg/m^3	μ_L = 1.3 10^{-2} kg/(m·s)	k = 0.145
λ_L = 77 W/(m·K)	Δh_f = 3.97 10^5 J/kg	m = -344 K
λ_S = 153 W/(m·K)	D_L^{Cu} = 5 10^{-9} m^2/s	T_E = 821.35 K
$c_{P,L}$ = 1179 J/(kg·K)	D_S^{Cu} = 8 10^{-13} m^2/s	

Table 1: Material properties used for the simulation.

Computations for the two-dimensional simulations were performed on a grid that contains 40 control volumes in the *x*-direction and 40 in the *y*-direction. A variable time step control was implemented to ensure convergence in all situations. The calculations were performed on an SGI-Octane workstation. Computations similar to the one presented in Fig.2 - 4 took about 3 hours.

The presented two-phase model reveals three empirical parameters, g_α, g_{Eut} and K_0. The major aim of this work was to investigate the impact of two of these parameters on the dynamics of the solid movement and on the evolution of the solidification process. Four cases are compared in which g_α and K_0 are varied. As the presented results concern only the beginning of the solidification process, g_{Eut} was kept constant. Table 2 defines the four different cases by summarizing the parameters used.

	Case A	Case B	Case C	Case D
g_α [Kg/(m^3·s·K)]	10^4	10^4	10^4	10^3
g_{Eut} [Kg/(m^3·s·K)]	10^2	10^2	10^2	10^2
K_0 [m^2]	$8{\cdot}10^{-11}$	$8{\cdot}10^{-10}$	$8{\cdot}10^{-9}$	$8{\cdot}10^{-11}$

Table 2: Summary of the simulation parameters.

Figure 2 shows the temporal evolution of u_s and u_l for case A. Due to the heat extraction, the solidification starts at the left wall. The dense solid immediately sinks and drags along the liquid. This causes a anti-clockwise vortex in the liquid. However this vortex is strongly influenced by the moving solid: As the solid is too heavy to flow around in the stream of the liquid vortex, it moves along the bottom wall, which then widens the liquid vortex. Only when the solid hits the opposite wall, it follows the vortex stream upwards. However, after a short time this upwards movement is stopped due to the loss of momentum. The stagnancy of the solid phase leads to a stagnancy of the liquid phase in the same region. As a consequence, the liquid vortex becomes narrow again. Generally it can be stated, that in case A the momentum transfer between liquid and solid phase is so high, that both velocity fields are strongly coupled.

Figure 3 shows T, α_s, c_l, u_s and M_{sl} at Δt = 6sec for case A and B. In Figure 4 the same quantities at Δt = 10sec are shown. From these figures the following observations can be made: (i) Solute redistribution due to solidification leads to an enrichment of the melt. (ii) Both, the temperature distribution and the species distribution in the liquid are effected by the movement of the solid (and liquid) phase. (iii) The solid phase flows into regions where remelting conditions exist. (iv) Because of the fact that the liquid flow distributes solute, a relative movement between liquid and solid causes a solute enrichment in regions without solid.

The influence of a weak or strong mechanical coupling between the liquid and the solid phase on the flow pattern can be seen by comparing case A, B and C. In case A the coupling is strong and thus the flow patterns of the liquid and the solid phase are almost equal. In case C where only a weak coupling is assumed, quite high relative velocities between liquid and solid appear. From the comparison of the three cases, the following statements can be made. (i) In all cases the sinking solid drags along the liquid and thus causes the liquid anti-clockwise vortex. (ii) The maximum liquid velocity (in the vicinity of the left wall) is comparable for the three cases. However, with weak coupling the solid can sink even more freely, resulting in a larger sinking velocity compared with the liquid. (iii) With weak coupling the solid does not follow the liquid vortex stream upwards. (iv) The stronger the coupling the larger the remelting area at the front of the moving solid. (v) In cases of weak coupling, liquid enriched with solute is transported in regions without any solid. For comparison, Figures 3 and 4 show the differences in T, α_s, c_l, u_s and M_{sl} for case A and B at two different times.

Finally in case D the mass transfer parameter g_α has been reduced by one order of magnitude compared to case A. However this change had no noticeable impact on the considered solidification process. The reason is that the mass transfer rate M_{ls} is governed by the heat extraction only. A change in g_α results then in a different deviation from equilibrium expressed in terms of $(c_l^{Cu^*} - c_l^{Cu})$ (Eq.(6)). In the considered cases $M_{ls} \approx 1$ kg/(m^3·s) and with g_α taken as in case A and C, the difference between the equilibrium concentration $c_l^{Cu^*}$ and the average concentration c_l^{Cu} is approximately 10^{-4}-10^{-3}. Therefore, practically c_l^{Cu} follows the phase diagram in both cases.

4. Conclusions

The main conclusions of this work are:

- A simple two-phase approach can give important insights into the dynamics which occur during the solidification of equiaxed growing alloys.
- A weak or a strong mechanical coupling between the liquid and the solid phase leads to different evolutions in $T, \alpha_s, c_l, c_s, u_s$ and u_l. Therefore, the formulation which describes the momentum transfer between liquid and solid is important and should be addressed in future research work.
- The mass transfer rate is governed by heat extraction. Sophisticated models for the mass transfer are thus not of significant importance.

Acknowledgement

This research was sponsored by the German Science Foundation (DFG) within the framework of the collaborative research center SFB 370 for which the authors wish to express their gratitude. We are also grateful to Dr. Braun of Fluent Germany for his support in handling software problems.

References

[1] C. Beckermann, C.Y. Wang, 3. Chapter in "Annual Review of Heat Transfer", Vol. 6, ed.: C.L. Tien (1995) pp. 115
[2] C. Beckermann, JOM (1997) pp. 13
[3] I.M. Krieger, Adv. Colloid Interf. Sci. B (1972) pp.111
[4] R.J. Feller, C. Beckermann, Metall. Trans., Vol. 28B (1997) pp. 1165
[5] C.Y. Wang, S. Ahuja, C. Beckermann, H.C. de Groh III, Metall. Trans., Vol. 26B (1995) pp. 111
[6] M. Hassanizadeh, W. Gray, Adv. Water Resources, Vol. 3 (1980) pp. 25
[7] R.B. Bird, W.E. Stewart, E.N. Lightfoot, in "Transport Phenomena", John Wiley & Sons, New York, NY (1960)
[8] S.V. Patankar. Numerical Heat Transfer and Fluid Flow, McGraw-Hill, New York (1980)

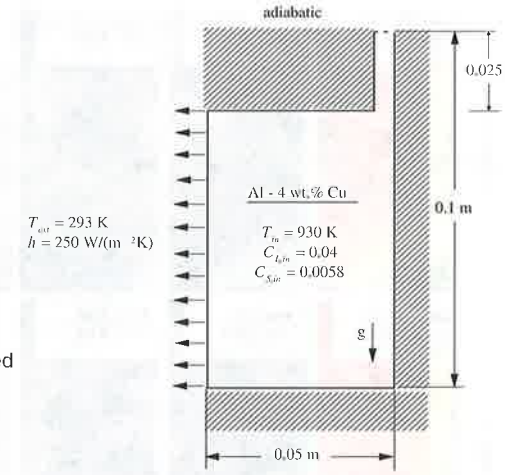

Figure 1: Schematic drawing of the physical system used in the simulation. The domain is divided into 40 increments in each direction.

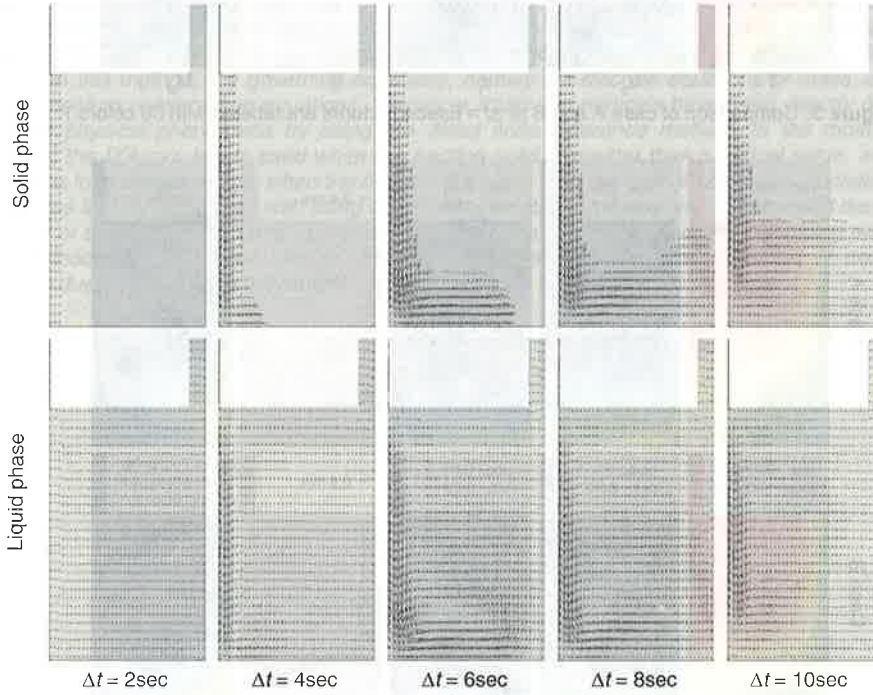

Figure 2: Velocity fields of the solid (a) and liquid phase (b) at different times for case A. (Maximum length of the arrows: 0.4 m/s)

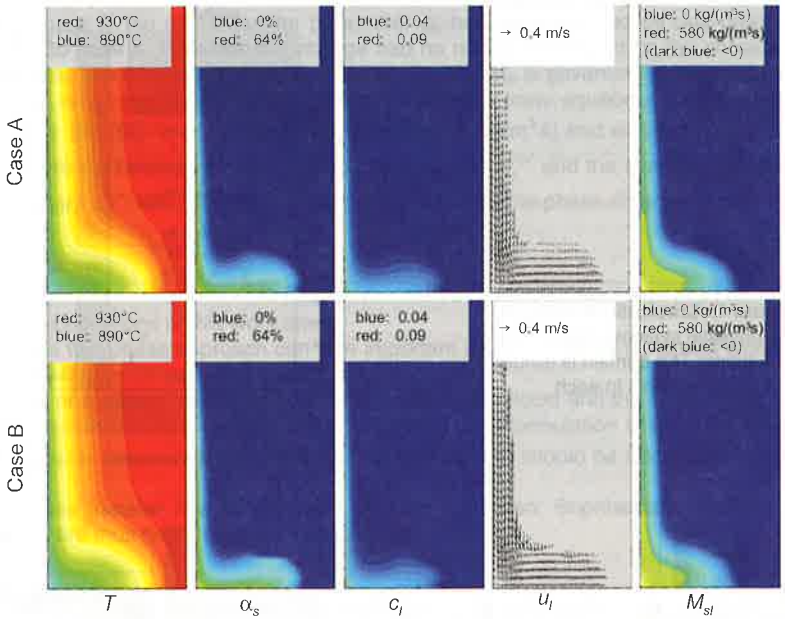

Figure 3: Comparison of case A and B at Δt = 6sec. (Pictures are labeled with 30 colors.)

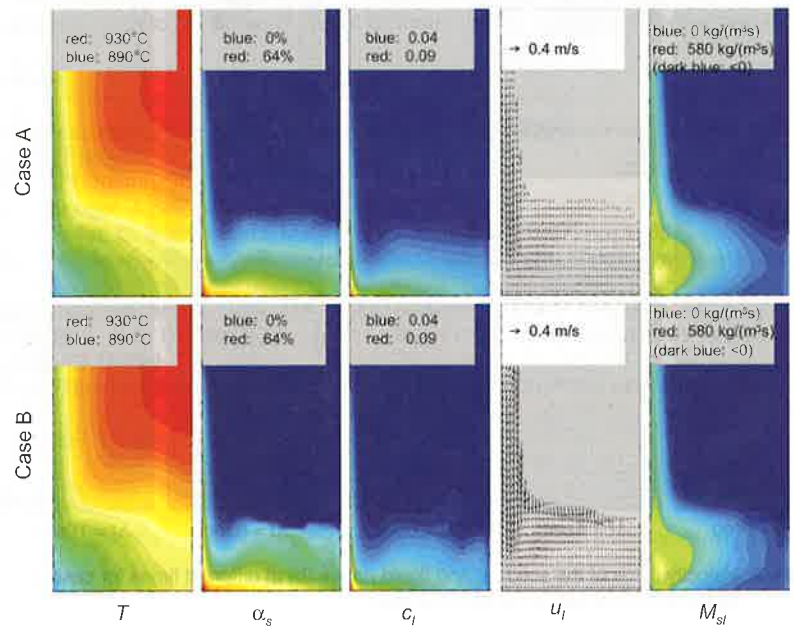

Figure 4: Comparison of case A and B at Δt = 10sec. (Pictures are labeled with 30 colors.)